Chapter 10

Design of Polymer Extrusion Dies Using Finite Element Analysis

G.N. Kouzilos, G.V. Seretis, C.G. Provatidis and D.E. Manolakos

Additional information is available at the end of the chapter

http://dx.doi.org/10.5772/intechopen.72211

Abstract

A computational fluid dynamics (CFD) model has been developed to compute the pressure, temperature, velocity, viscosity and viscous dissipation in the high-density polyethylene (HDPE) extrusion process. The numerical approach agrees fairly well with the experimental data recorded during the extrusion process of the material. The extrusion spider die was designed to produce high-density polyethylene pipes of 32 mm inner nominal diameter and 2.4 mm thickness. In order to investigate if the spider legs are able to perform under the pressure occurred using the maximum flow rate provided by the single screw extruder of this study, a stress analysis was conducted on a single spider leg. This fluid-structure interaction (FSI) problem was solved using the COMSOL Multiphysics software. Finally, the results obtained from the FE analysis were applied in the design and fabrication of the spider die, selecting IMPAX (tool steel) as fabrication material.

Keywords: finite element analysis, pressure flow, HDPE, extrusion die, spider, arbitrary Lagrangian-Eulerian (ALE)

1. Introduction

The production of extruded polyethylene film, rods, tubes and pipes is a common industrial process that has been the subject of major investigations over many years [1–3]. The designing of extrusion dies for the production of such geometries requires a deep knowledge. It is usually based on experimental trial-and-error approaches, involving, therefore, the use of huge

amounts of time and material resources [4–6]. According to manufacturers, 10–15 iterations are required to optimize complex profile geometries [1]. The extrusion die is one of the most important parts in extrusion processing. The extrusion die design process can become too difficult to execute, or its cost can increase up to prohibitive levels, when complex geometry thermoplastic profiles are concerned.

Optimizing process parameter problems is routinely performed in the manufacturing industry, particularly in setting final optimal process parameters. Final optimal process parameter setting is recognized as one of the most important steps in plastics extrusion for improving the quality of extruded products.

Yilmaz et al. [7] optimized the geometric parameters of a profile extrusion die, using several objective function definitions by Simulated Annealing-Kriging Meta-Algorithm. Objective functions are defined based on the uniformity of velocity distribution at the die exit. For this, computational fluid dynamics (CFD) simulations are performed for N = 70 die geometries. Appropriate geometric parameters (t and L) of the die are variables for the optimization problem.

The optimization of an extrusion die designed for the production of a wood-plastic composite (WPC) decking profile is investigated by Gonçalves et al. [8]. The optimization was performed with the help of numerical tools, more precisely, by solving the continuity and momentum conservation equations that govern such a flow, and aiming to balance properly the flow distribution at the extrusion die flow channel outlet.

A nonlinear optimization technique was applied by Mamalis et al. [9] to the numerical model to pinpoint the processing conditions, namely inlet pressure, inlet temperature of the melt, temperature of the die walls and temperature of the spider legs.

The work described, hereinafter, is aiming to the development of an optimum design for a pipe die with spider used for the extrusion of high-density polyethylene (HDPE) tubes. For this purpose, a computational fluid dynamics (CFD)-based model using the generalized Newtonian approach was employed to investigate pressure drop, flow and temperature uniformity in the die.

2. Extrusion die design zones

In order to determine the die pressure, that is, the pressure developed in the inner surfaces of the die, the analytical approach, which is presented below, was used. The extrusion die was considered to consist of five different zones. In each zone, a different stage of the extrusion process was taking place. In zone 1, the fluid enters the die (input or inlet). In zone 2, the fluid diverts from the extrusion axis. In this stage of the extrusion process, the distribution of the fluid begins on the top of the mandrel cone and, subsequently, the fluid is driven to zone 3 through a ring-shaped leak. In zone 3, the fluid is leaking in the spider legs, which are fitting in the male end of the die. A relaxation zone (zone 4) follows zone 3. The last stage is zone 5,

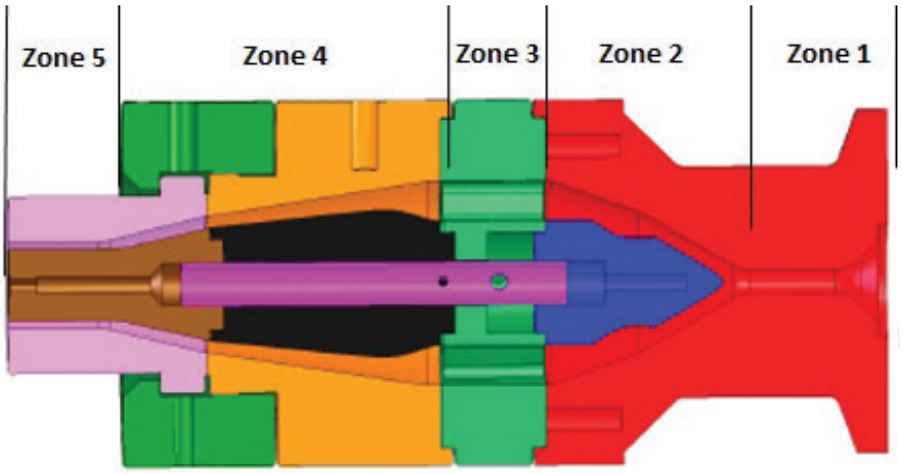

Figure 1. Zones of the extrusion die.

where the pipe is being formed at its expected morphological characteristics. The extrusion die zones are presented schematically in **Figure 1**.

3. Mathematical model

In order to determine the pressure drop in the extrusion die, the power-law exponential model was used, according to which the volumetric flow rate $\dot{V}$ of a non-Newtonian fluid is described by Eqs. (1) and (2) [1, 2].

$$\dot{V} = K' \cdot \varphi \cdot \Delta P^m \tag{1}$$

where φ is the fluidity, m is the flow exponent, ΔP is the pressure drop and K' is a die shape constant.

For the present work, a single-screw Johnson Plastics extruder was used to drive the flowing high-density polyethylene into the spider die. For this kind of extruder, the volumetric flow rate, as it has been described previously [2], is

$$\dot{V} = \alpha \cdot \mathrm{N} - \frac{\beta}{\mu}\frac{\Delta P}{L} \tag{2}$$

where $\alpha = 0.5 \cdot \pi^2 \cdot D^2 \cdot H \cdot \sin\phi \cdot \cos\phi$, N is the screw speed, $\beta = \frac{\pi}{12} D \cdot H^3 \cdot \sin^2\phi$, μ is the melt viscosity, L is the axial length of the screw, D is the inner barrel diameter, H is the depth of the channel and φ is the helix angle of flight [10].

In the five different zones of the extrusion die, three shapes of the cross section can be found: tube, ring shape and square shape. For these cross sections, the pressure drop is described by Eqs. (3)–(5), respectively [1, 10].

$$\Delta P_{tube} = L\left[\frac{2^{m}(m+3)\,\dot{V}}{\varphi \cdot \pi \cdot R^{m+3}}\right]^{1/m} \tag{3}$$

$$\Delta P_{ring} = L\left[\frac{2^{m+1}(m+2)\,\dot{V}}{\phi \cdot \pi \cdot D \cdot H^{m+2}}\right]^{1/m} \tag{4}$$

$$\Delta P_{square} = L\left[\frac{2^{m+1}(m+2)\,\dot{V}}{\phi \cdot B \cdot H^{m+2}}\right]^{1/m} \tag{5}$$

These equations have broad applications because the flow path in a small segment of many extrusions dies and adaptors can be approximated by a circular tube or a slit for the purpose of calculating pressure drop and flow rate. For a zero value of ΔP, the volumetric flow rate is maximized. Thus, for screw speed equal to 100 rpm, the maximum volumetric flow rate can be calculated equal to 7.9×10^{-6} m^3/s.

For this flow rate, the total drop of the pressure in the die ΔP_T, including all five different zones, is:

$$\Delta P_T = \Delta P_{Zone1} + \Delta P_{Zone2} + \Delta P_{Zone3} + \Delta P_{Zone4} + \Delta P_{Zone5} = 17.9\ bar + 9.55\ bar + 1.58\ bar + 27.34\ bar + 35.8 = 92.17\ bar \tag{6}$$

If ΔP_T is the total drop of the die pressure and ρ and C_p are the density and the specific heat, respectively, then the average temperature increase at the die output (outlet), which is based on the assumption that adiabatic conditions occur throughout the whole process, can be expressed by Eq. (7) [2].

$$\Delta T_{analytical} = \frac{\Delta P}{\rho \cdot C_p} = 4.72\ \mathrm{K} \tag{7}$$

4. Design of the extrusion die

The extrusion die was designed to produce high-density polyethylene pipes of 32 mm inner nominal diameter and 2.4 mm thickness. The material used for the body of the extrusion die was IMPAX steel. The extrusion die was assembled in five stages. Progressive views of the assembly process are presented in **Figure 2**.

A 3D view of the die along with the screw type used is given in **Figure 3**.

Firstly, the spider head was combined with the male middle mandrel. Subsequently, the outer mandrel and the torpedo were placed in the initial assembly. In stage 3, the die housing was added, and in the following stage (stage 4), the middle ring was adapted to the back side of the spider head. In the last stage (stage 5), the die ring was combined with the middle ring of the previous stage.

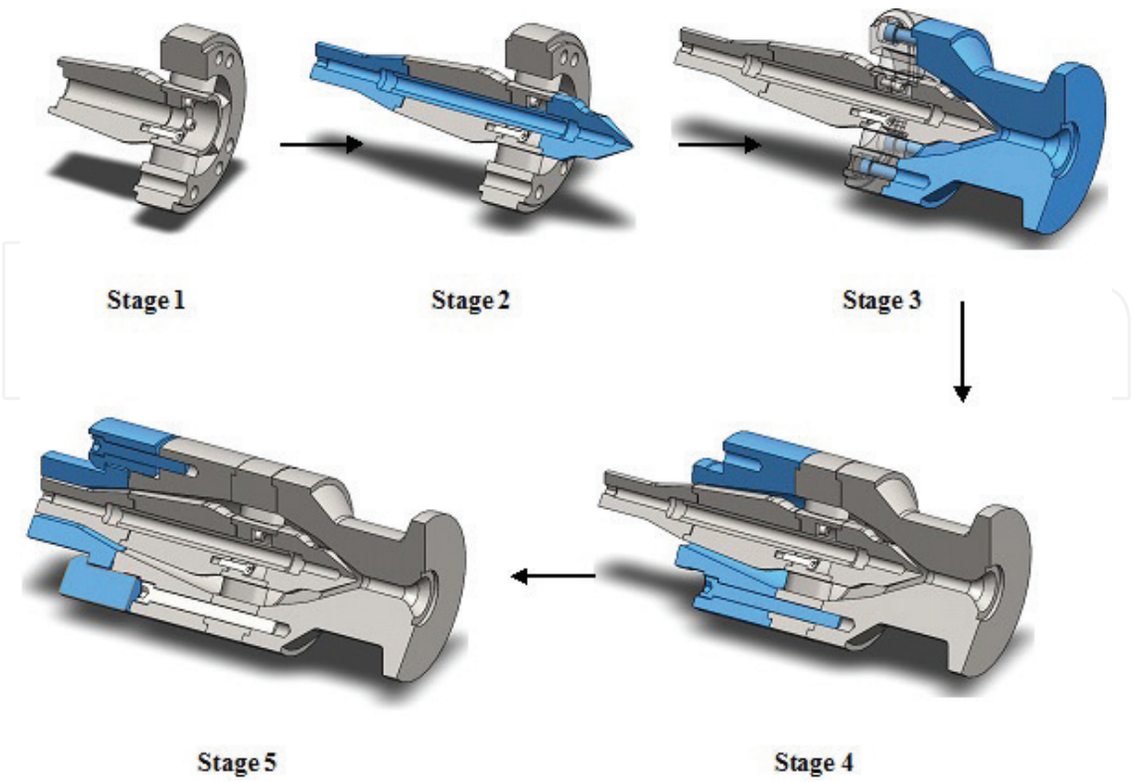

Figure 2. Progressive view of the complete assembly process.

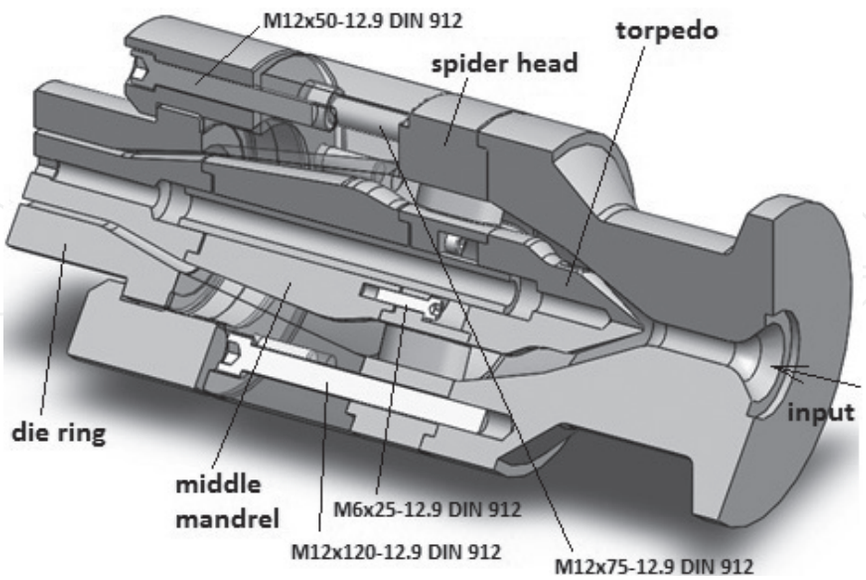

Figure 3. 3D view of the spider extrusion die.

5. Finite element analysis

5.1. CFD analysis

A three-dimensional conjugate heat transfer model, which has been developed for non-Newtonian materials, was processed in the extrusion die. For the numerical solution, the following consideration had been made: a homogeneous and isotropic high-density polyethylene (HDPE) melt with a uniform temperature of T = 469 K is flowing into the spider die. The temperature of the die surface was kept constant at the value T_w = 469 K, and the volumetric flow rate of the polymer melt was fixed at $\dot{V}_{max} = 7.9 \times 10^{-6}\, m^3/s$.

In most polymer processes, the elastic memory effects can hardly be observed and, therefore, it can be ignored. Since this chapter is concentrated on a qualitative analysis of the flow regimes, the inelastic model was selected as the most appropriate in terms of describing the melt flow.

Due to the polymer melts flow characteristics when it takes place in an extrusion die channel while in steady state, the following assumptions have been made:

- Incompressible steady laminar flow.
- Since the Reynolds number of the melts' flow is extremely low, inertial and gravitational forces are neglected.
- No slipping on the wall interface.
- Uniform and constant die temperature, equal to 469 K.
- Constant volumetric flow rate, equal to 7.9×10^{-6} m^3/s.

The inlet (input), the outlet (output) and the die wall are presented in **Figure 4**.

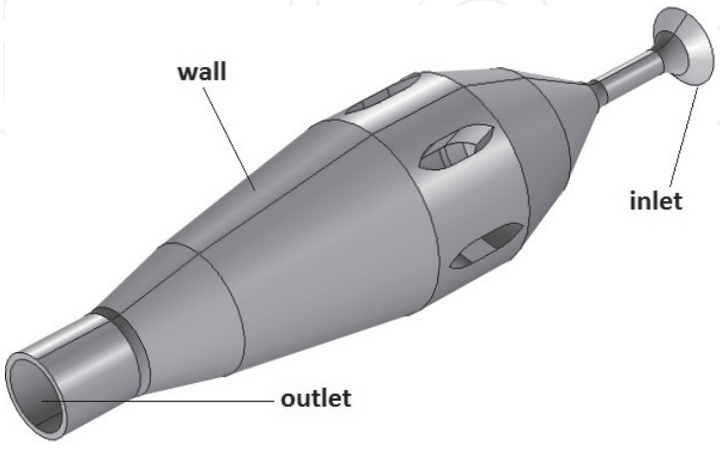

Figure 4. Inner die model used in numerical analysis.

Since the polymer melts are non-Newtonian fluids, the Carreau-Yasuda model was selected to describe dependence of the viscosity on the shear rate and temperature [3]. This model is presented in Eq. (8).

$$n = a_T \cdot n_0(T_R)\left[1 + \left(a_T \cdot \dot{\lambda}(T_R)\,\dot{\gamma}\right)^{\alpha}\right]^{(n-4)/\alpha} \tag{8}$$

where a_T is the shift factor and n_0, λ, α and n are model's fitting parameters.

If ∇ is the Hamilton differential operator, u is the velocity vector, T is the temperature, C_p is the heat capacity and Q is the total source term, the governing equations of the model used can be written in the form below [2, 3]:

$$\text{Continuity equation: } \nabla u = 0 \tag{9}$$

$$\text{Motion equation: } \nabla \sigma = 0 \tag{10}$$

$$\text{Energy equation: } \rho \cdot C_p \cdot u \cdot T = -\nabla q + Q \tag{11}$$

The Cauchy stress vector is given in Eq. (12).

$$\sigma = -p \cdot I + S \tag{12}$$

where p, S and I are the hydrostatic pressure, the extra stress tensor and the Kronecker delta, respectively.

The CFD code of COMSOL 4.3b, using Carreau-Yasuda viscosity model, was used to solve the governing equations. For this model, the effect of the viscous dissipation, that is, the shear heating effect, which is responsible for the fluid temperature increase, was taken into account. This is quite important in polymer extrusion processes and their design.

In order to create the fluid domain, the flow simulation add-in of SolidWorks was used and two lids were created, one in the inlet and another in the outlet of extrusion die as shown in **Figure 5(b)** and **(c)**. Then, the fluid body assembly was created, choosing all the parts of the extrusion die as shown in **Figure 5(d)**. Finally, after deleting all the unneeded subparts, the fluid domain was taken as shown in **Figure 5(e)**.

The mesh model used for the simulations is presented in **Figure 5(f)**. This model included 95,215 tetrahedral finite elements, and the minimum and maximum element sizes were 5.56×10^{-4} and 13×10^{-3} mm, respectively. This mesh was created using automated unstructured mesh generator.

The finite element analysis results for the temperature distribution are presented in **Figure 6(a)**. These results were obtained using the energy balance equations in different positions of the die domain. The input temperature, that is, the temperature of the polymer melt when it enters the die domain, was 469 K. Due to the viscous dissipation, this temperature progressively

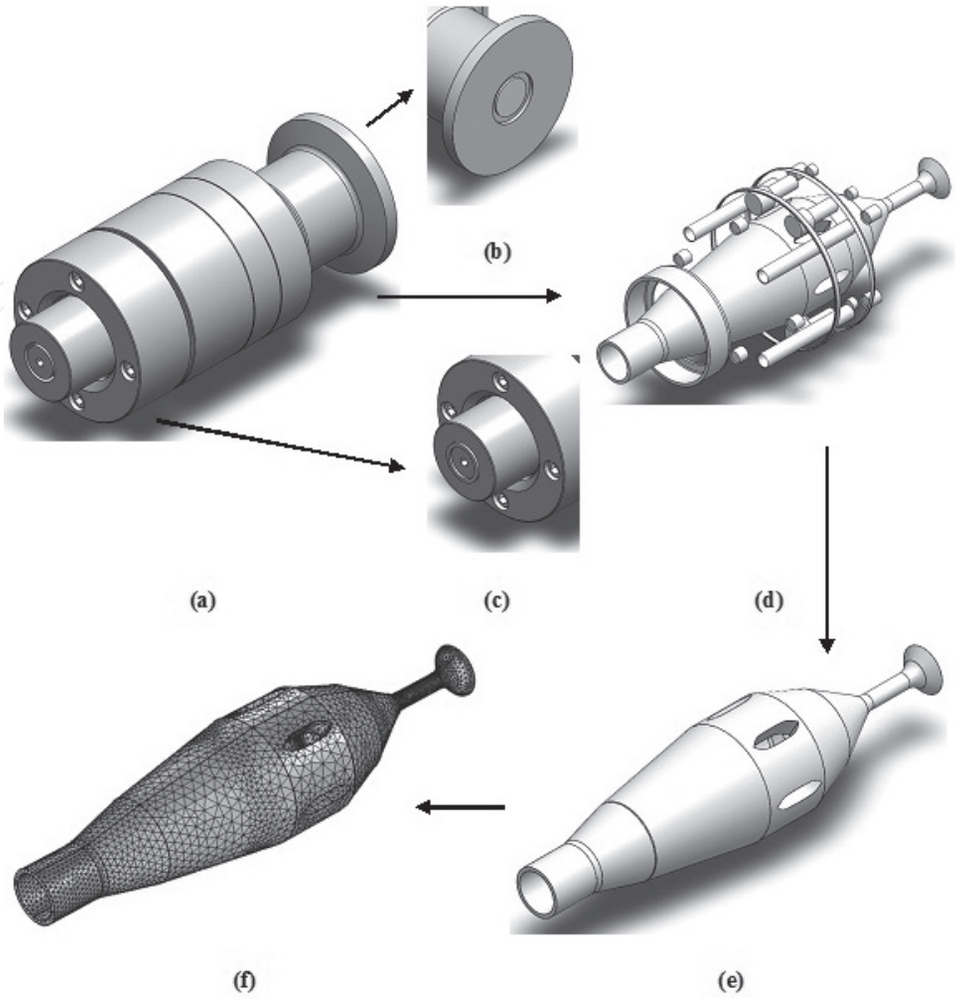

Figure 5. Steps for the geometrical model design (a)–(e) and mesh model of the domain (f).

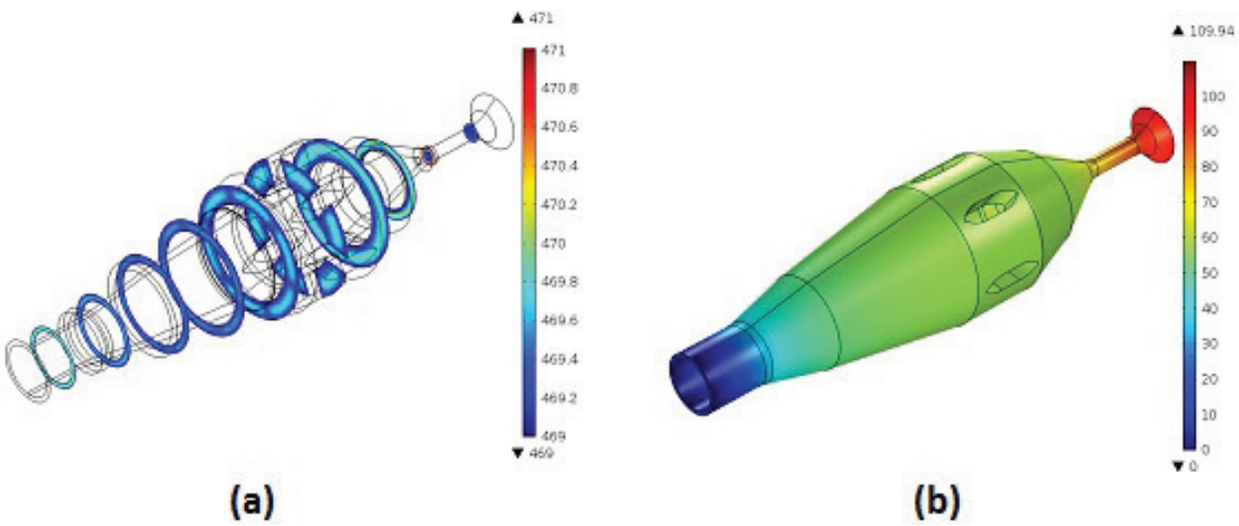

Figure 6. Finite element analysis results for the die domain.

increases, while the flow is moving toward the outlet. The average temperature of the polymer melt is given by Eq. (13) [2], and its increase calculated is equal to 1.53 K.

$$T = \frac{\int_s T \cdot u \cdot ds}{\int_s u \cdot ds} \tag{13}$$

The respective value for the temperature increase calculated using the mathematical model, that is, 4.72 K, was considerably greater in comparison with the finite element analysis results. This is due to the simplification assumption used for the mathematical analysis which indicated that the die walls are adiabatic. In practice, this consideration of the adiabatic wall facilitates the solving process of the mathematical model, but it considerably affects the temperature increase value.

The results of the finite element analysis performed as regards the pressure distribution on the die domain are presented in **Figure 6(b)**. It is obvious that the pressure follows a reduction trend while moving from the extrusion die inlet to its outlet. The pressure drop calculated using finite element analysis was 97.24 bar. This value was similar to the one calculated using the mathematical model, that is, 92.17 bar (Eq. (6)).

5.2. Fluid-structure interaction analysis of the spider head

The most crucial parts of such an extrusion die, as regards its failure under pressure, are the spider legs. The so-called parts of the spider head are the thickest parts of the whole structure, and consequently, these are the most possible points for failure onset under pressure. Therefore, if a single spider leg is able to perform under a specific pressure without failure, it is safe for the whole structure to perform under this pressure.

In order to investigate if the spider legs are able to perform under the pressure occurred using the maximum flow rate provided by the single-screw extruder of this study, a stress analysis was conducted on a single spider leg. This fluid-structure interaction (FSI) problem was solved using the COMSOL Multiphysics software. The solid mechanics continuum equations (Eq. (14)), together with the fluid mechanics Navier-Stokes equations (Eq. (15), were solved using the arbitrary Lagrangian-Eulerian (ALE) method. The deforming geometry dynamics were applied on the boundaries of the moving grid (mesh), and new mesh coordinates were calculated on the channel for each moving step of the boundaries. These moving mesh coordinates were applied on the Navier-Stokes equations. Fixed coordinates were used for the structural parts of the model, that is, for the nonfluid parts, since the strain of these parts was calculated by the COMSOL Multiphysics using structural mechanics. The calculation of the deformed coordinates using ALE formulation was based on the calculated strain of the structural parts.

$$-\nabla \cdot u = 0 \tag{14}$$

$$\rho \frac{\partial u}{\partial t} - \nabla \cdot \left[-p \cdot I + \eta(\nabla u + (\nabla u)^T)\right] + \rho(u \cdot \nabla)u = F \tag{15}$$

In Eq. (15), I is the unit diagonal matrix and F is the volume force which affects the fluid.

Eq. (15), that is, Navier-Stokes, if solved for the velocity u and the pressure p, describes the fluid flow in the channel. Gravitation is not taken under consideration in this model. The same goes for the volume force which affects the fluid. Therefore, the value of the force F in Eq. (15) is equal to zero ($F = 0$). These equations are applied on the deformed coordinates.

The fluid flow at the inlet is described by a fully developed laminar flow and at the outlet is described by a noncompressible flow ($p = 0$). No-slipping conditions, that is, $u = 0$, were applied on the rest of the boundaries.

An elastic and nonlinear model was used in order to apply the large displacement method on the structural domain. Fixed support was applied on the lower and upper spider head boundaries (ring geometry), which indicates an ability lack for movement toward any direction.

The spider head examined is presented in **Figure 7**. In the same figure, the meshing types for the spider leg analysis can be found. The mesh of a single spider leg was unstructured, and it was constituted by 8732 tetrahedral elements. The minimum and maximum element sizes were 1.01×10^{-4} and 2.36×10^{-3} mm, respectively. The flow mesh was also unstructured and was constituted by 62,412 tetrahedral elements. The minimum and maximum element sizes for this type of mesh were 1.17×10^{-4} and 2.03×10^{-3} mm, respectively.

After the mesh-generating process, the solution of the numerical model took place. **Figure 8** presents the finite element analysis results for equivalent stress and total displacement. As can be observed in **Figure 8(a)**, the maximum flow rate of the extruder used leads to the development of a stress equal to 14.79×10^{-2} MPa, which is the maximum stress that can be achieved for HDPE flow with the specific extruder. On the other hand, the yield stress of the IMPAX tool steel used for the die parts is 8×10^{2} MPa. Since the maximum Von Misses equivalent

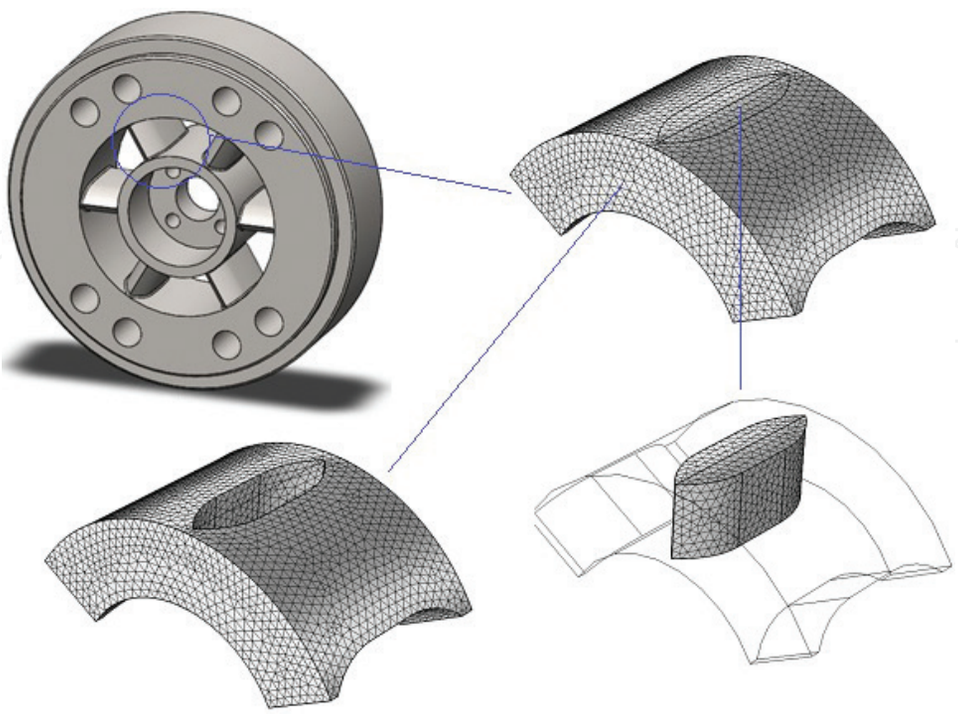

Figure 7. Spider head and mesh types of spider leg, fluid and their combination.

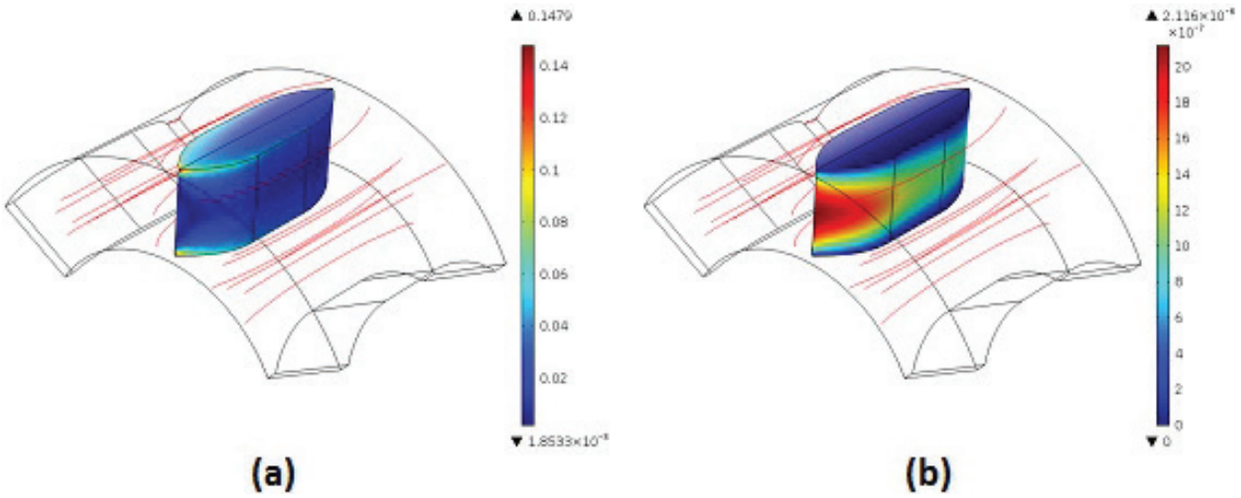

Figure 8. Von misses equivalent stress (a) and total displacement (b) developed on a single spider leg of the extrusion die's spider head.

stress is considerably lower than the yield stress of the spider leg material, the designed spider head, and consequently the entire die, is effective for extrusion processes with the specific single-screw extruder.

6. Manufacturing

The G-code used for the cutting processes applied for the production of each part was generated using SolidCAM software (CAM package). It was transmitted to the CNC cutting

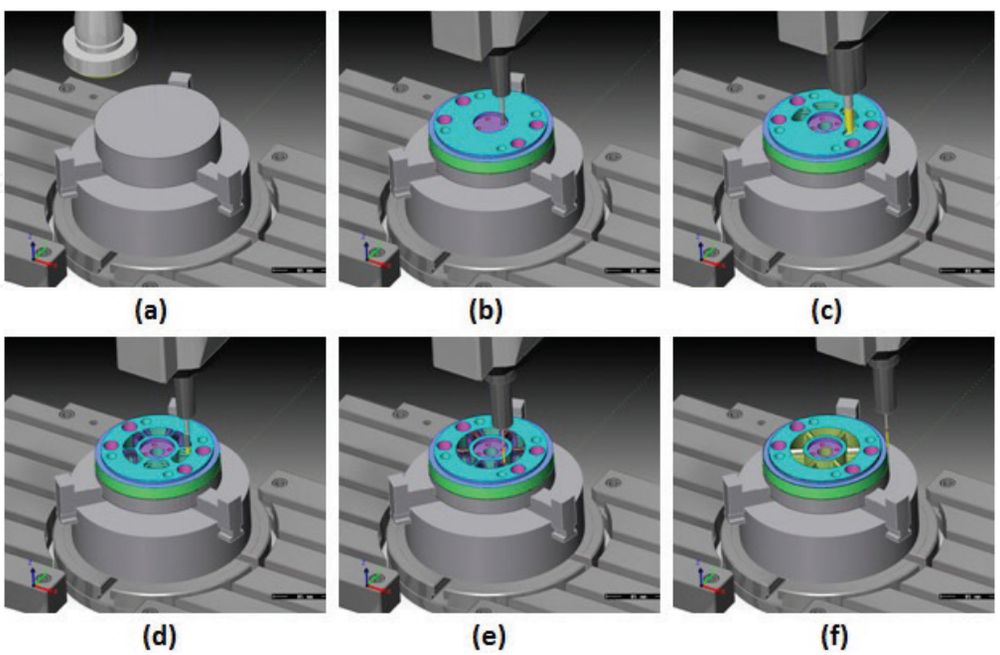

Figure 9. 3D simulation of the cutting process for the production of the spider head in SoliCAM environment.

Figure 10. Johnson Plastics single-screw extruder together with the mounted extrusion die.

machines used, an OKUMA MX-45VE CNC milling cutting center and an OKUMA LB10II CNC lathe, with DNC technology. The 3D simulation of the cutting process for the production of the spider head in SoliCAM environment is presented in **Figure 9**.

Since the spider die was intended to be used for the production of HDPE tubes, it was mounted on a single-screw Johnson Plastics extruder with characteristics: length/diameter ratio 24.1, screw diameter 38 mm and compression ratio 2.75. The extruder with the mounted extrusion die is presented in **Figure 10**.

7. Results and discussion

A summary of the analytical, experimental and numerical results reported in the current chapter including the pressure drop and temperature rise in the die is presented in **Table 1**. The calculated by the mathematical model pressure drop was approximately 3.3% lower than the actual (experimental) result [2]. This can be explained by the fact that the analytical model simplifies the pressure drop calculation in cases of complex geometries. However, the divergence of the calculated value is quite low. On the other hand, the maximum average temperature rise data show 174% divergence compared with the corresponding temperature obtained experimentally. This is due to the simplification assumption used for the mathematical analysis which indicated that the die walls are adiabatic.

The comparison between the experimental and non-Newtonian die flow simulations seems to reveal the expected good agreement with the overall pressure drop as well as with the constant wall temperature boundary conditions.

The pressure data calculated by the numerical Carreau-Yasuda model (97.24 bar) show a fairly good agreement with the experimental results (95.15 bar), whereas the average temperature rise of the molten HDPE was T = 1.53 K, which is approximately 11% higher than the experimental temperature value. This was the value calculated for the boundary conditions

	Mathematical model	Carreau-Yasuda (Numerical) Constant wall temperature	Carreau-Yasuda (Numerical) No heat flux	Experimental
dP (bar)	92.17	97.24	97.24	95.15
dT (K)	4.72	1.53	6.66	1.72
Error dP (%)	3.13	2.19	2.19	
Error dT (%)	174.42	11.05	287.21	

Table 1. Analytical, numerical and experimental data.

of wall with constant temperature. In the case of adiabatic boundary conditions, the average temperature rise of the molten HDPE was considerably higher than the experimental one.

Figure 11 presents the pressure drop throughout all the die zones and the total pressure drop (expressed as percentage) calculated using the mathematical model (**Figure 11(a, b)**) and finite element analysis (**Figure 11(c, d)**). It is obvious that the majority of the pressure drop is observed along the zone V, at the exit of extrusion die.

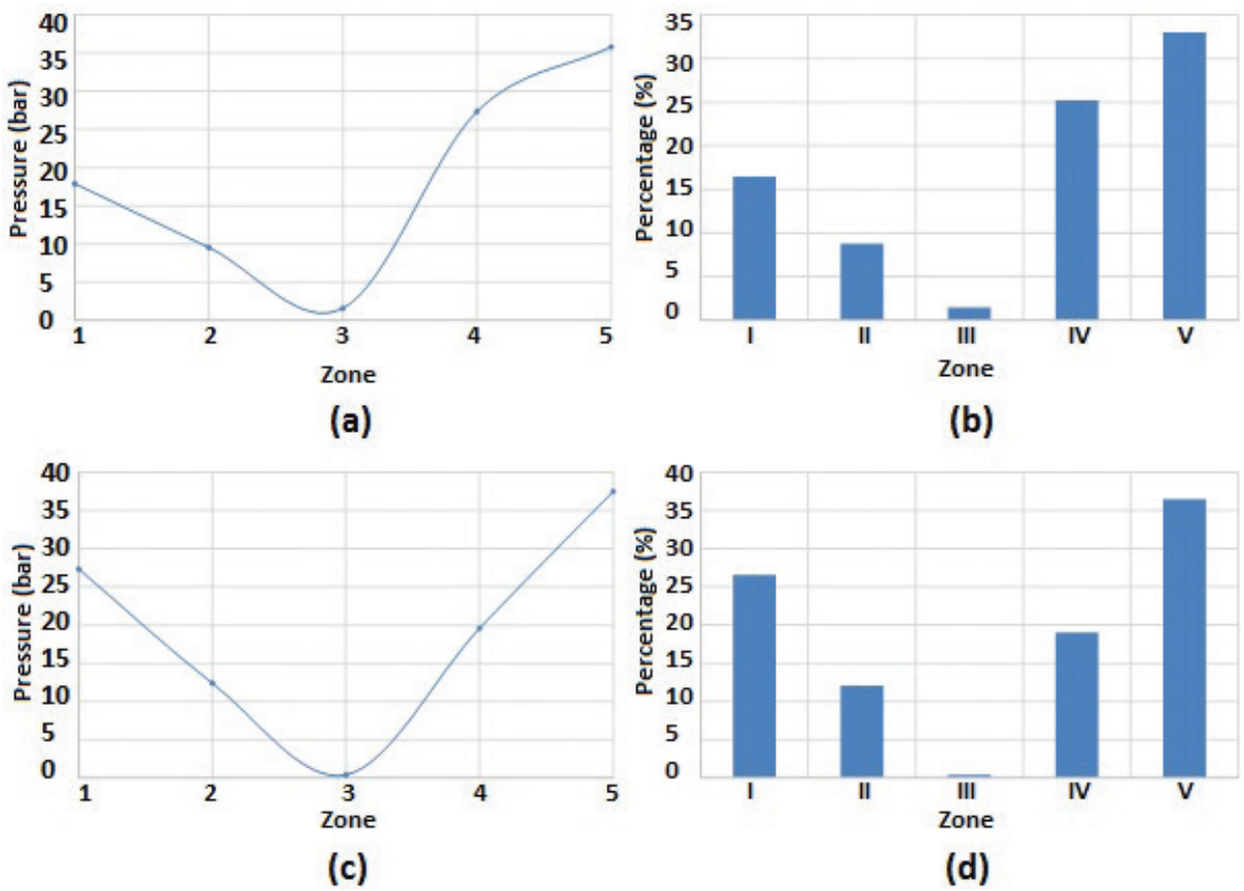

Figure 11. Pressure drop throughout the die zones and total pressure drop calculated using the mathematical model (a, b) and finite element analysis (c, d).

The calculated, using finite element analysis, Von Misses equivalent stresses are significantly lower than the yield stress of the die material, and therefore, it may be concluded that the abovementioned tool steel is suitable for manufacturing spider dies for polymer extrusion applications.

8. Conclusions

Summarizing the main features of the results reported, it may be concluded that there is a significant difference comparing the numerical and analytical models with regard to the temperature developed in the fluid during the extrusion process. This can be explained by the fact that the analytical model is based on the assumption that adiabatic conditions occur, which means that there is no heat transfer between the wall and the polymer material as described above. Finally, it was demonstrated by the stress analysis that the die construction is strong enough to withstand the pressure developed during the die operation and that the stresses do not exceed the material yield strength in any case.

Author details

G.N. Kouzilos*, G.V. Seretis, C.G. Provatidis and D.E. Manolakos

*Address all correspondence to: gkouzilosb@yahoo.com

National Technical University of Athens, School of Mechanical Engineering, Athens, Greece

References

[1] Michaeli W. Extrusion Dies for Plastics and Rubber: Design and Engineering Computations. 3rd ed. Munich: Carl Hanser Verlag GmbH & Co. KG; 2003. p. 362. DOI: 10.3139/9783446401815

[2] Kouzilos GN, Markopoulos AP, Manolakos DE. Manufacturing and modeling of an extrusion die spider head for the production of HDPE tubes. Journal of Manufacturing Technology Research. 2015;**6**(1-2):1-15

[3] Mamalis AG, Kouzilos G, Vortselas AK. Design feature sensitivity analysis in a numerical model of an extrusion spider die. Journal of Applied Polymer Science. 2011;**122**(6):3537-3543. DOI: 10.1002/app.34762

[4] Choudhary MK, Kulkarni JA. Modeling of three-dimensional flow and heat transfer in polystyrene foam extrusion dies. Polymer Engineering & Science. 2008;**48**(6):1177-1182. DOI: 10.1002/pen.20990

[5] Lebaala N, Schmidtb F, Puissanta S. Design and optimization of three-dimensional extrusion dies, using constraint optimization algorithm. Finite Elements in Analysis and Design. 2009;**45**(5):333-340. DOI: 10.1016/j.finel.2008.10.008

[6] Huang GQ, Huang HX. Optimizing Parison thickness for extrusion blow molding by hybrid method. Journal of Materials Processing Technology. 2007;**182**(1-3):512-518. DOI: 10.1016/j.jmatprotec.2006.09.015

[7] Yilmaz O, Gunes H, Kirkkopru K. Optimization of a profile extrusion die for flow balance. Fibers and Polymers. 2014;**15**(4):753-761. DOI: 10.1007/s12221-014-0753-3

[8] Gonçalves ND, Teixeira P, Ferrás LL, Afonso AM, Nóbrega JM, Carneiro OS. Design and optimization of an extrusion die for the production of wood–plastic composite profiles. Polymer Engineering & Science. 2015;**55**(8):1849-1855. DOI: 10.1002/pen.24024

[9] Mamalis AG, Vortselas AK, Kouzilos G. Tube extrusion of polymeric materials: Optimization of the processing parameters. Journal of Applied Polymer Science. 2012;**126**(1):186-193. DOI: 10.1002/app.36555

[10] Rauwendaal C. Polymer Extrusion. 5th ed. Munich: Carl Hanser Verlag GmbH & Co. KG; 2014. p. 950. DOI: 10.3139/9781569905395

IntechOpen